Journal of Solid Mechanics Vol. 5, No. 1 (2013) pp. 22-34

Flow-Induced Instability Smart Control of Elastically Coupled Double-Nanotube-Systems

V. Atabakhshian[1], A. Ghorbanpour Arani[2,3*], A.R. Shajari[2], S. Amir[2]

[1]*Department of Mechanical Engineering, Faculty of Engineering, Bu-Ali Sina University, Hamedan, Iran*
[2]*Faculty of Mechanical Engineering, University of Kashan, Kashan, Islamic Republic of Iran*
[3]*Institute of Nanoscience & Nanotechnology, University of Kashan, Kashan, Islamic Republic of Iran*

Received 13 January 2013; accepted 28 February 2013

ABSTRACT

Flow induced vibration and smart control of elastically coupled double-nanotube-systems (CDNTSs) are investigated based on Eringen's nonlocal elasticity theory and Euler-Bernoulli beam model. The CDNTS is considered to be composed of Carbon Nanotube (CNT) and Boron-Nitride Nanotube (BNNT) which are attached by Pasternak media. The BNNT is subjected to an applied voltage in the axial direction which actuates on instability control of CNT conveying nano-fluid. Polynomial modal expansions are employed for displacement components and electric potential and discretized governing equations of motion are derived by minimizing total energies of the CDNTS with respect to time-dependent variables of the modal expansions. The state-space matrix is implemented to solve the eigen-value problem of motion equations and examine frequencies of the CDNTS. It is found that Pasternak media and applied voltage have considerable effects on the vibration behavior and stability of the system. Also, it is found that trend of figures have good agreement with the other studies. The results of this study can be used for design of CDNTS in nano / Micro -electro-mechanical systems.

Keywords: Double-nanotube system; Instability smart control; Pasternak media; Conveying nano-fluid

1 INTRODUCTION

THE Boron-Nitride nanotubes (BNNTs) discovered in the mid 1990s, are extensively utilized in the nano-electro-mechanical (NEMS) and micro-electro-mechanical systems (MEMS) in recent years, according to the unique structural properties. Possessing strong piezoelectric characteristic, high elastic modulus and superb structural stability respect to Carbon nanotubes (CNTs) are important properties of BNNTs that hasn't observed in the other nanostructures [1]. Hence, the wide applications of the BNNTs in the nano sensors and actuators and reinforcement in the nano-composites can be mentioned here briefly [2-4].

Buckling of BNNTs with zigzag atomic structure under combined electro-thermo-mechanical loadings was investigated by Salehi-Khojin and Jalili [5]. They suggested that the zigzag structure of BNNTs have longitudinal piezoelectricity property and are more stable for axial loadings. Ghorbanpour Arani et al. [6] studied the electro-thermo-mechanical vibration response of BNNTs. They used nonlocal Timoshenko beam theory in their analysis which was not considered for BNNTs in the existed literature.

Regarding nano and micro structures conveying fluid, analysis of nonlinear vibration of the fluid-conveyed CNTs were studied by Kuang et al. [7]. The various aspects of nonlinearity conditions of the considered model were

* Corresponding author. Tel.: +98 913 162 6594; Fax: +98 361 591 2424.
E-mail address: aghorban@kashanu.ac.ir (A.Ghorbanpour Arani).

investigated on the vibration responses of the system and it was found that coupling between longitudinal and transverse coordinates has significant effect on the amplitude–frequency properties. Fu et al. [8] studied on the nonlinear vibration of the embedded CNTs and discussed on the effects of the surrounding elastic medium, van der Waals forces and aspect ratio of the CNT on the amplitude frequency response characteristics.In order to consider fluid-scale in the nano-structures, validity of the classical fluid velocity profile in nanotubes is assessed by Narasimhan [9].

One of the most important nano-structures is CDNTS that includes connected two or more nanotubes [10]. The atomic interactions between nanotubes in the CDNTS are considered often by Van der Waals force and elastic medium [11]. The nonlocal effects of the double-nanorod systems on the axial vibration were researched by Murmu and Adhikari [12]. In the numerical analysis, they considered nanorod to be CNT and concluded that the fundamental natural frequency of axially vibrating nanorods has a decreasing nature with the increasing nonlocal parameter.

In this study, flow-induced instability of a CDNTS, consisting BNNT and CNT which are coupled by Pasternak media is investigated. The nanotubes are modeled as nonlocal Euler-Bernoulli beam and steady-state fluid flow is considered to be conveyed through the CNT. In order to achieve an active control on the vibration response of the system, external electric potential is imposed on the BNNT and considerable effects are observed in this regard. This study is commonly used as reference of the CDNTS investigations in NEMS.

2 NONLOCAL PIEZOELASTICITY THEORY

Based on the theory of nonlocal piezoelasticity, the stress and the electric displacement at a reference point x depend not only on the components of the strain and electric-field at the same position, but also on all other points of the body. The nonlocal constitutive equations for BNNT as a piezoelectric material in the occupied region of the body V, can be given as follows [13]:

$$\sigma_{ij}^{BN}(\mathrm{x}) = \int_V \alpha\left(|\mathrm{x}-\mathrm{x}'|,\tau\right) t_{ij}^{BN}(\mathrm{x}')\mathrm{dV}(\mathrm{x}'), \qquad \forall \mathrm{x} \in \mathrm{V} \tag{1a}$$

$$D_i^{BN}(\mathrm{x}) = \int_V \alpha\left(|\mathrm{x}-\mathrm{x}'|,\tau\right) \Delta_i^{BN}(\mathrm{x}')\mathrm{dV}(\mathrm{x}'), \qquad \forall \mathrm{x} \in \mathrm{V} \tag{1b}$$

and for the CNT, we have

$$\sigma_{ij}^{C}(\mathrm{x}) = \int_V \alpha\left(|\mathrm{x}-\mathrm{x}'|,\tau\right) t_{ij}^{C}(\mathrm{x}')\mathrm{dV}(\mathrm{x}'), \qquad \forall \mathrm{x} \in \mathrm{V} \tag{2}$$

where σ_{ij} and D_i are the components of nonlocal stress and electric displacement tensors, respectively, and superscript *BN* indicate boron-nitride and C indicate carbon nanotube. The kernel function $\alpha\left(|\mathrm{x}-\mathrm{x}'|,\tau\right)$ is the nonlocal modulus, $|\mathrm{x}-\mathrm{x}'|$ is the Euclidean distance, and $\tau = e_0 a / l$ is defined as the scale coefficient that incorporates the small scale factor, where e_0 is a constant appropriate to each material and a and l are the internal and external characteristic length (e.g. crack length, wavelength), respectively. In addition, t_{ij} and Δ_i imply classical stress and classical electric displacement, respectively. According to axially polarization of BNNT controller, the nonlocal constitutive equations for BNNT and CNT can be written as [14]:

$$\left(1-(e_0 a)^2\nabla^2\right)\sigma_{ij}^{BN} = t_{ij}^{BN}, \tag{3a}$$

$$\left(1-(e_0 a)^2\nabla^2\right)D_{ij}^{BN} = \Delta_{ij}^{BN}, \tag{3b}$$

$$\left(1-(e_0 a)^2\nabla^2\right)\sigma_{ij}^{C} = t_{ij}^{C}, \tag{4}$$

where ∇^2 represents the Laplace operator. The above implicit relations couple the nonlocalstress and electric displacement with the classical stress and electric displacement.To achieve explicit relations, an iterative-based method can be suggested for the above equations as follows:

$$\left\{\sigma_{ij}\right\}^{k+1} = \left(e_0 a\right)^2 \nabla^2 \left\{\sigma_{ij}\right\}^k + \left\{t_{ij}\right\}, \tag{5a}$$

$$\left\{D_{ij}\right\}^{k+1} = \left(e_0 a\right)^2 \nabla^2 \left\{D_{ij}\right\}^k + \left\{\Delta_{ij}\right\}, \tag{5b}$$

where k is the iteration number and the first iteration can be started by local results. It is clear that accuracy of the nonlocal results will be improved by increasing the number of iterations.

3 MODELING OF THE PROBLEM

Consider a vertically coupled nonlocal nanotube system as shown in Fig 1. In the present study, the CNT containing steady nano-flow is controlled by a parallel BNNT which is subjected to external electric voltage $\delta\varphi_0$ in axial direction. The CNT and BNNT are attached by longitudinal and vertical springs which are simulated by Pasternak foundation theory that is capable of both transverse shear loads (G_p) and normal loads (K_w). Based on Euler-Bernoullibeam model, the components of axial and transverse displacement (i.e., $\tilde{u}(x,z,t)$ and $\tilde{w}(x,z,t)$) for CNT and BNNT are expressed as:

$$\begin{cases} \tilde{u}^i(x,z,t) = u^i(x,t) - z\dfrac{\partial w^i(x,t)}{\partial x} & i:C \ \ or \ \ BN \\ \tilde{w}^i(x,z,t) = w^i(x,t) \end{cases} \tag{6}$$

u and w are the components of the middle surface displacement (i.e., displacement at $z=0$) and additionally x and z are the coordinates taken along the length and the thickness of the beam. Hence, the strain-displacement relationship is given by:

$$\varepsilon_x^i = \frac{\partial u^i}{\partial x} - z\frac{\partial^2 w^i}{\partial x^2} \quad i:C \ \ or \ \ BN. \tag{7}$$

The classical constitutive relations of stress and electric displacement for BNNT are expressed as:

$$t_x^{BN} = C_{11}^{BN}\varepsilon_x^{BN} - e_{11}E_x - \lambda_1^{BN}\Delta T, \tag{8a}$$

$$\Delta_x^{BN} = e_{11}\varepsilon_x^{BN} - \in_{11} E_x - p_1\Delta T, \tag{8b}$$

where $C_{11}, e_{11}, \in_{11}, \lambda_1$ and p_1 denote elastic, piezoelectric, dielectric, pyroelectric coefficients and thermal modulus, respectively. And for the CNT, we have

$$t_x^C = C_{11}^C\varepsilon_x^C - \lambda_1^C\Delta T. \tag{9}$$

where $C_{11}, e_{11}, \in_{11}, \lambda_1$ and p_1 denote elastic, piezoelectric, dielectric, pyroelectric coefficients and thermal modulus, respectively. Also, the unidirectional electric field along the axial direction of BNNT in terms of electric potential φ is reduced as:

$$E_x = -\frac{\partial\varphi}{\partial x}. \tag{10}$$

The Eqs. (8) to (9) should be inserted into nonlocal equations (Eqs. (5)), in order to evaluate small scale effects of the CDNTS.

4 ENERGY FUNCTIONS

The total elastic strain energy of CDNTS is consists of elastic strain energy of BNNT subjected to axial electric field and CNT as:

$$U^{BN} = \frac{1}{2}\int_0^L \int_{A_{BN}} \left(\varepsilon_x^{BN}\sigma_x^{BN} - D_x E_x\right) dA^{BN}\, dx, \tag{11}$$

$$U^{C} = \frac{1}{2}\int_0^L \int_{A_C} \varepsilon_x^{C}\sigma_x^{C}\, dA^{C}\, dx. \tag{12}$$

The kinetic energy of BNNT and CNT, are given by [15]

$$T^i = \frac{1}{2}\rho^i \int_0^L \int_{A^i} \left[\left(\frac{\partial u^i}{\partial t} - z\left(\frac{\partial^2 w^i}{\partial x \partial t}\right)\right)^2 + \left(\frac{\partial w^i}{\partial t}\right)^2\right] dA^i dx, \quad i: C \ \ or \ \ BN. \tag{13}$$

Often, the fluid structures interaction problems are considered by the assumption of no-slip boundary conditions, although this assumption is no longer valid for nano size problems due to consideration of the small-scale effects and the *Kn* effects. In this regard, Rashidi et al. [16], suggested an average flow velocity correction factor (VCF) as follows:

$$VCF \triangleq \frac{V_{avg,slip}}{V_{avg,no-slip}} = \left(4\left(\frac{2-\sigma_\upsilon}{\sigma_\upsilon}\right)\left(\frac{Kn}{1+Kn}\right)+1\right), \tag{14}$$

where σ_υ is tangential momentum accommodation coefficient and is taken equal with 0.7 for most practical purposes [17], and Kn is the Knudsen number. It is noted that for the nano-liquid-flow against with nono-gas flow the *Kn* is so small that the effects of viscosity can be ignored. Hence, from now on, we may substitute velocity field for slip boundary condition by applying VCF on velocity field for no-slip boundary condition.

The kinetic energy associated with the fluid flow is expressed as [15]

$$T_f = \frac{1}{2}\rho_f \int_0^L \int_{A_f} \left(VCF^2\left(\vec{V}_{no-slip}.\vec{V}_{no-slip}\right) + z^2\left(\frac{\partial^2 w^C}{\partial x \partial t}\right)^2\right) dA_f\, dx. \tag{15}$$

where $\vec{V}_{no-slip}$ is the fluid velocity vector can be written as:

$$\vec{V}_{no-slip} = \left(U_f \cos\gamma + \frac{\partial u^C}{\partial t}\right)\hat{i} + \left(-U_f \sin\gamma + \frac{\partial w^C}{\partial t}\right)\hat{j},$$
$$\gamma = -\frac{\partial w^C}{\partial x}. \tag{16}$$

where U_f is velocity of fluid in CNT. Total energy associated with external works including Pasternak foundation between nanotubes and the fluid flow is given by [15]

$$W = W_{Pasternak} + W_{fluid} = -\frac{1}{2}\int_0^L \left(K_w w^r - G_p \nabla^2 w^r \right) w^r dx$$
$$+\frac{1}{2}\int_0^L m_f \left(VCF.V_{no-slip} \right)^2 \frac{\partial^2 w^C}{\partial x^2} w^C \cos\gamma \, dx - \frac{1}{2}\int_0^L m_f \left(VCF.V_{no-slip} \right)^2 \frac{\partial^2 w^C}{\partial x^2} u^C \sin\gamma dx; \quad (17)$$

where $w^r = w^C - w^{BN}$, and $m_f = \rho_f A_f$ is the mass density of fluid per unit length.

5 MODAL EXPANSION ANALYSIS

The dimensionless parameters used in this study are defined as:

$$(\bar{u}^i, \bar{w}^i) = \frac{(u^i, w^i)}{h_i} \ , \ \xi = \frac{x}{L} \ , \ K^*_w = K_w / E^C \ , \ G^*_p = G_p / E^C Rh \ , \quad (18)$$
$$\Omega = \omega L \sqrt{\rho_C / E^C} \ , \ U^*_f = U_f \sqrt{\rho_f / E^C} \ .$$

Simply supported geometric boundary conditions are considered for the BNNT and CNT as:

$$\begin{cases} \bar{w}^i(0,t) = \bar{w}^i(1,t) = 0 \\ \bar{w}''^i(0,t) = \bar{w}''^i(1,t) = 0, \quad i: C \ \ or \ \ BN. \\ \bar{u}^i(0,t) = \bar{u}^i(1,t) = 0 \end{cases} \quad (19)$$

The displacement components $\bar{u}^i$ and $\bar{w}^i$ can be expanded by following expression (say trial functions), which satisfy the geometric boundary conditions (19) of the CDNTS at both ends [18].

$$\bar{u}^C = \sum_{j=1}^{N} \Pi_j(t) \xi^j (1-\xi) \quad , \quad \bar{w}^C = \sum_{j=1}^{N} \Upsilon_j(t) \xi^j (1-\xi) \quad ,$$
$$\bar{u}^{BN} = \sum_{j=1}^{N} \Xi_j(t) \xi^j (1-\xi) \quad , \quad \bar{w}^{BN} = \sum_{j=1}^{N} \Gamma_j(t) \xi^j (1-\xi) \quad , \quad (20)$$

where $\Pi_j(t)$, $\Upsilon_j(t)$, $\Xi_j(t)$ and $\Gamma_j(t)$ are time-variant functions and N is the summation integer that can be increased to obtain maximum accuracy and acceptable results.

Considering longitudinal polarization, the function of electric potential ϕ may be expanded as following expression:

$$\varphi = \delta\varphi_0 (1-\xi) + \sum_{i=1}^{N} \Phi_j \xi^j (1-\xi) \quad (21)$$

where Φ_j is the constant amplitude components of the electric potential and $\delta\varphi_0$ is the imposed electric potential on the BNNT cotroller.

Denoting the unknown dynamic displacement and potential vector:

$$\{\eta\}_{5N} = [\underbrace{\{\Pi_j\},\{\Upsilon_j\},\{\Xi_j\},\{\Gamma_j\}}_{\eta_d},\underbrace{\{\Phi_j\}}_{\eta_\phi}]^T \quad , \quad j = 1,2,...,N \tag{22}$$

where $\{\eta_d\}$ and $\{\eta_\varphi\}$ introduced respectively, the dynamical displacement and amplitude of electric potential vectors. Hence, the dimension of $\{\eta_d\}$ is $4N$ and may be explained as the number of degrees of freedom (DOFs) of the system used in the modal expansions.

The Lagrange equations of motion for the CDNTS are:

$$\frac{d}{dt}\left[\frac{\partial(T_C + T_{BN} + T_F)}{\partial \dot{\eta}_k}\right] - \frac{\partial(T_C + T_{BN} + T_F)}{\partial \eta_k} + \frac{\partial(U_C + U_{BN})}{\partial \eta_k} = \frac{\partial W}{\partial \eta_k} \quad , \quad k = 1,..., 5N \tag{23}$$

Using mode expansions (20) and (21), all the terms in Eq.(23) are evaluated and a system of discretized governing equations is obtained in matrix form as follows:

$$[M]\{\ddot{\eta}\} + [C]\{\dot{\eta}\} + [K]\{\eta\} = \{0\}, \tag{24}$$

where $[M], [C]$ and $[K]$ are the mass, damping and stiffness matrices, respectively.

The governing equations (Eq. (24)) can be separated for dynamic displacement and potential displacement as:

$$\begin{bmatrix} M_{dd} & 0 \\ 0 & 0 \end{bmatrix}\begin{Bmatrix} \ddot{\eta}_d \\ \ddot{\eta}_\varphi \end{Bmatrix} + \begin{bmatrix} C_{dd} & 0 \\ 0 & 0 \end{bmatrix}\begin{Bmatrix} \dot{\eta}_d \\ \dot{\eta}_\varphi \end{Bmatrix} + \begin{bmatrix} K_{dd} & K_{d\varphi} \\ K_{\varphi d} & K_{\varphi\varphi} \end{bmatrix}\begin{Bmatrix} \eta_d \\ \eta_\varphi \end{Bmatrix} = \{0\} \tag{25}$$

Due to existence of static coupling between mechanical and electric displacement, the parts of mass and damping matrices associated with $\dot{\eta}_\varphi$ and $\ddot{\eta}_\varphi$ are obtained zero. By means of second set of equations of Eq. (25), the amplitude of electric field vector can be calculated in terms of displacement vector:

$$\{\eta_\varphi\} = -\left[K_{\varphi\varphi}^{-1}\ K_{\varphi d}\right]\{\eta_d\} \tag{26}$$

Eliminating η_φ in Eq. (25) and using Eq. (26), yields the modified equations of motion as:

$$[M_{dd}]\{\ddot{\eta}_d\} + [C_{dd}]\{\dot{\eta}_d\} + [K_M]\{\eta_d\} = \{0\} \tag{27}$$

where

$$K_M = K_{dd} - K_{d\phi} K_{\phi\phi}^{-1} K_{\phi d}. \tag{28}$$

Introducing new vectors $y_1 = \eta_d$ and $y_2 = \dot{\eta}_d$, the modified equations of motion can be written in the following state-space form as:

$$\frac{d}{dt}\begin{Bmatrix} y_1 \\ y_2 \end{Bmatrix} = \begin{bmatrix} 0 & \mathrm{I} \\ -M_{dd}^{-1} K_m & -M_{dd}^{-1} C_{dd} \end{bmatrix}\begin{Bmatrix} y_1 \\ y_2 \end{Bmatrix} \tag{29}$$

The general solution of Eq. (27) can be expressed as:

$$\{y_1, y_2\} = \{\hat{y}_1, \hat{y}_2\}\exp(\Omega t) \tag{30}$$

where Ω is complex circular frequency containing imaginary and real parts denoting natural and damping frequencies, respectively and $\{\hat{y}_1, \hat{y}_2\}$ are amplitudes of the displacements vector and their time derivatives. Applying Eq. (30) in Eq. (29), yields

$$\Omega \begin{Bmatrix} \hat{y}_1 \\ \hat{y}_2 \end{Bmatrix} = \begin{bmatrix} 0 & \mathrm{I} \\ -M_{dd}^{-1} K_M & -M_{dd}^{-1} C_{dd} \end{bmatrix} \begin{Bmatrix} \hat{y}_1 \\ \hat{y}_2 \end{Bmatrix} \tag{31}$$

where eigenvalues of the state-space matrix are complex frequencies of the system.

6 RESULTS AND DISCUSSION

In this section, instability of CDNTS being attached by an elastic media is discussed so that the effects of nonlocal parameter, Kn number, mode number, coupled media constants,aspect ratio and external applied voltage on the dimensionless natural and damping frequencies of CNT are also considered.The parallel nanotubes are considered to be the same length and the simply supported boundary conditions as shown in Fig. 1. The mechanical properties of CNT as well as mechanical and electrical properties of BNNT are listed in Table 1. [19-20]. The radius, of BNNT r^{BN} and CNT r^{C} are taken as $11.43\,nm$ and $0.7\,nm$, respectively. The length of the nanotubes is taken as $20\,nm$ and the thicknesses are taken as $0.075\,nm$ and $0.34\,nm$, respectively for BNNT and CNT. Additionally, in order to generalize the problem, a range of low to high spring stiffness as different elastic medium must be considered. The internal fluid flow density ρ is taken as $1000\,Kg/m^3$.

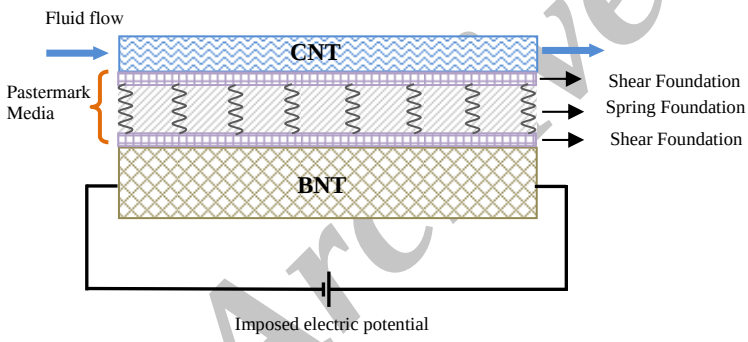

Fig. 1
Schematic representation of the coupled nanotube system conveying fluid flow.

Table 1
DNTS mechanical and electrical properties

BNNT	SWCNT (5,5)
$E = 1.8(TPa)$	$E = 0.971(TPa)$
$\upsilon = 0.34$	$\upsilon = 0.3$
$e_{11} = 0.95(C/m^2)$	$\rho = 2500\,Kg/m^3$
$\lambda_1 = 2.44\times10^6\ (N/m^2K)$	
$\rho = 2300\,Kg/m^3$	

The variations of imaginary part of frequency known as natural frequency versus flow velocity for first three modes and various summation integers N in dimensionless forms are shown in Fig. 2. The solid lines, dashed lines and dotted lines used in this figure describe the results of summation integer 8, 6 and 4, respectively. It can be found that the result obtained by $N=4$ is valid only for 1st mode and is acceptable for 2nd mode in lower flow velocity. The results obtained by $N=6$ and 8 similarly show that by increasing the summation integer N, the up to $N/2$ of the first modes may be accurate and it is more exact for lower flow velocities asbeing expected. This discussion can be observed in Table 2 . for critical flow velocities. From now on and for more accuracy, the number of summation integer N is taken as 8. Fig. 2. also showsthat the natural frequency is decreased with increasing flow velocity for all modes until reaching the value zero and specially for 1st mode at $U_{d1}^{*}=0046$; in this case, a pitchfork bifurcation (divergence instability) occurs due to having a real part of complex frequency (damping frequency) that leads to amplifying the amplitude of vibration by absorbing the energy of the CNTs internal flow. After zero-frequency area the natural frequency becomes increased again and the stability of the system is restored in $U_{r1}^{*}=0.0093$. Once more for the second time the instability occurs (Flutter instability) by reaching the natural frequency value to $U_{d2}^{*}=0.0137$.

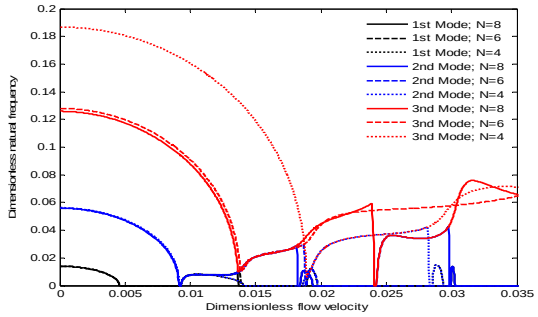

Fig. 2
Convergence of dimensionless natural frequency versus dimensionless flow velocity for first three modes by increasing the summation integer N.

Table 2
Comparison of the results for various modes and summation integer

	Mode 1			Mode 2			Mode 3		
N	U_{d1}^{*}	U_{r1}^{*}	U_{d2}^{*}	U_{d1}^{*}	U_{r1}^{*}	U_{d2}^{*}	U_{d1}^{*}	U_{r1}^{*}	U_{d2}^{*}
4	0.0046	0.0093	0.0141	0.0091	0.0141	0.0186	0.0189	---	---
6	0.0046	0.0093	0.0139	0.0091	0.0188	0.0198	0.0138	---	---
8	0.0046	0.0093	0.0137	0.0092	0.0182	0.0194	0.0137	0.0241	---
10	0.0046	0.0093	0.0137	0.0092	0.0182	0.0194	0.0137	0.0241	---

The effects of elastically coupled media are examined in Figs. 3-4 for both Winkler and Pasternak foundations. Figs. 3(a) and 3(b) show dimensionless natural and damping frequencies versus Winkler spring modulus for various flow velocities. It is observed that increasing Winkler modulus increases natural frequency as well as first critical flow velocity (divergence instability, U_{d1}^{*}) of the coupled CNT in the fundamental mode. In addition, the variations of natural and damping frequencies versus various flow velocities for different Pasternak modulus are drown in Figs. 4(a) and 4(b). As expected, increasing elastic media constant can improve the stability of the CDNTS by increasing the critical flow velocity of the fundamental vibration mode. From this figure, it is seen that the effect of elastic foundation with Pasternak model, is same as Winkler model qualitatively but higher difference is observed in second instability (U_{d2}^{*}). The main difference between these two types of media is observed that the Pasternak foundation is considerably more effective than the Winkler foundation in higher flow velocity as shown in U_{r1}^{*} and U_{d2}^{*}.

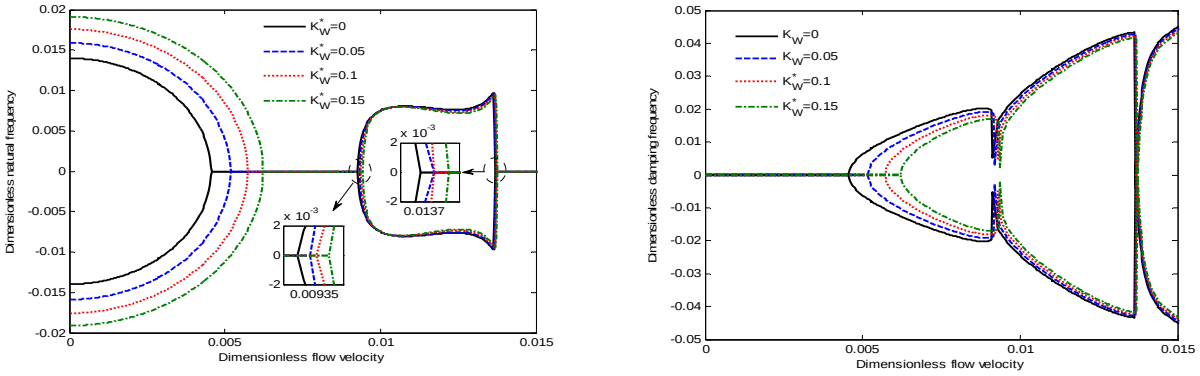

(a) (b)

Fig. 3
a) Dimensionless natural frequency versus dimensionless flow velocity for various Winkler modulus. b) Dimensionless damping frequency versus dimensionless flow velocity for various Winkler modulus.

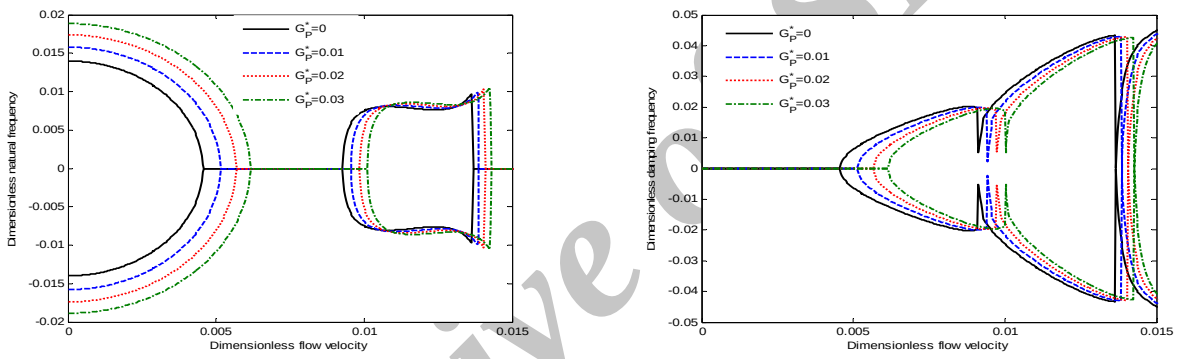

(a) (b)

Fig. 4
a) Dimensionless natural frequency versus dimensionless flow velocity for various Pasternak modulus. b) Dimensionless damping frequency versus dimensonless flow velocity for various Pasternak modulus.

Effect of small scale parameter on natural and damping frequency is investigated in Figs.5(a) and 5(b), respectively. It is found that increasing small scale leads to decrease divergence flow velocity inconsiderably as can be seen in zoomed sub graph. In addition, flutter instability area is smoothly decreased by increasing considerations of the small scale and it is more remarkable at higher flow velocities. From damping frequency variations respect to flow velocity, shown in Fig. 5(b), above discussion can be found, similarly.

Fig. 6(a) shows dimensionless natural frequency versus Kn, number for several modes. It is seen that with increasing Kn number the natural frequency is decreased for all modes and flutter instability which is defined for Figs. 6(a) and 6(b) can be observed also. A beat phenomenon between 1st and 2nd mode also observed from this figure and this is because of so small distance between mode 1 and 2 in the range of $Kn = 0.132$ to $Kn = 0.191$.

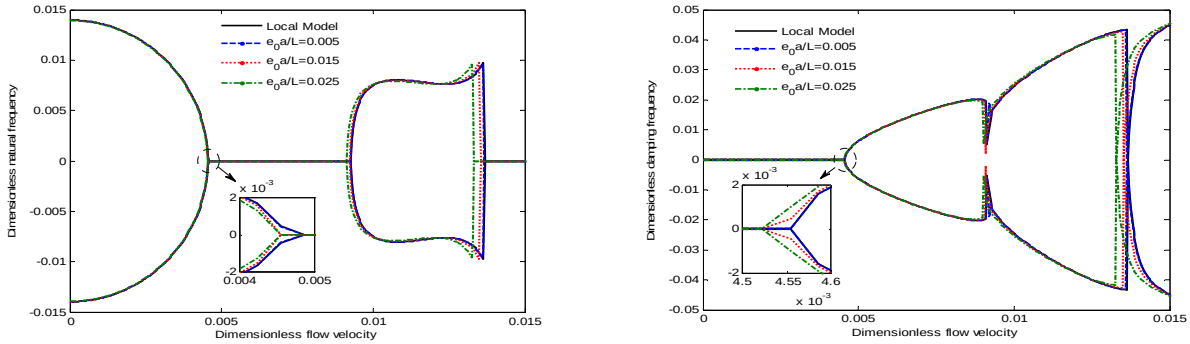

(a) (b)

Fig. 5
a) Effect of small-scale parameter on dimensionless natural frequency with changing flow velocity for 1st to 4st mode. b) Effect of small-scale parameter on dimensionless damping frequency with changing flow velocity for 1st to 4st mode.

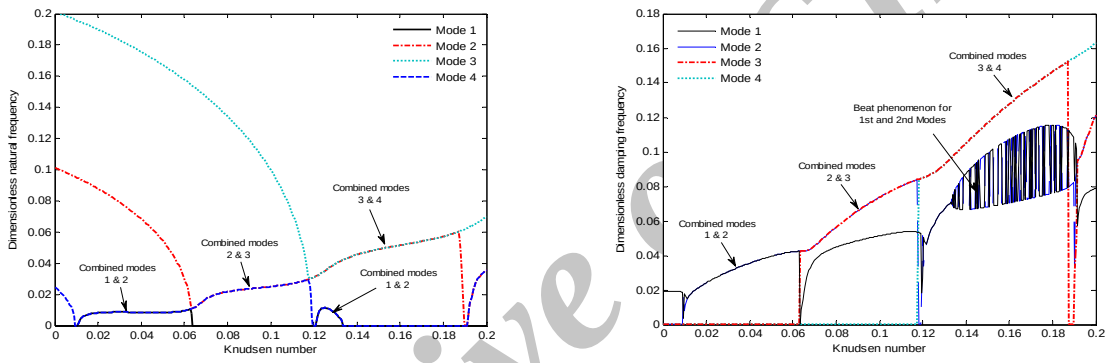

(a) (b)

Fig. 6
a) Dimensionless natural frequency versus Knudsen number for 1st to 4st mode. b) Dimensionless damping frequency versus Knudsen number for 1st to 4st mode.

Effects of external voltage and coupled media simultaneously are investigated in Figs. 7(a) and 7(b). As expected for elastic media, the stability of the system is increased by considering Winkler and Pasternak foundation. Regarding external voltage, it is observed that the system can be controlled by applying positive potential difference. The major effects of elastic media and external voltage can also be found in Fig. 7(b) which shows dimensionless damping frequency versus dimensionless flow velocity. On the other hand, quantitative investigation of elastic media constants together with applied voltage can be found in Figs.8 and 9.

Fig. 8 shows natural frequency versus Winkler modulus with and without considering external voltage. It is observed that applied voltage has major effect in mode 1 comparison to mode 2 and with increasing Winkler modulus, applied voltage becomes more considerable. Similarly for Pasternak modulus, same discussion can be found. The effect of aspect ratio on vibration response of the system is shown in Figs. 10(a)and 10(b). The variations of natural frequency versus aspect ratio for modes 1 to 4 is illustrated in Fig. 10(a). It is seen that for all modes, increasing aspect ratio decreases natural frequency until instability occurs in the system. This statement can be concluded from Fig. 10(b) also.

In order to validate results of the present study with other related publication, we comprise natural and damping frequency versus flow velocity with work of Kaviani and Mirdamadi [21] which investigated influence of Knudsen number on fluid viscosity for analysis of divergencein fluid conveying nano-tubes as shown in Figs. 11(a)and 11(b). Acceptable agreement can be observed from these figures.

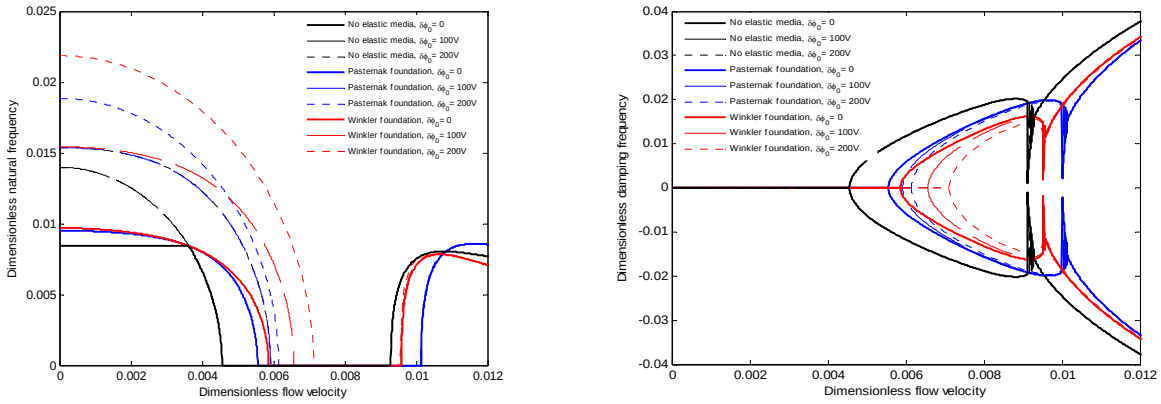

(a) (b)

Fig. 7
a) Dimensionless natural frequency versus dimensionless flow velocity for various magnitudes of imposed electric potential.
b) Dimensionless damping frequency versus dimensionless flow velocity for various magnitudes of imposed electric potential.

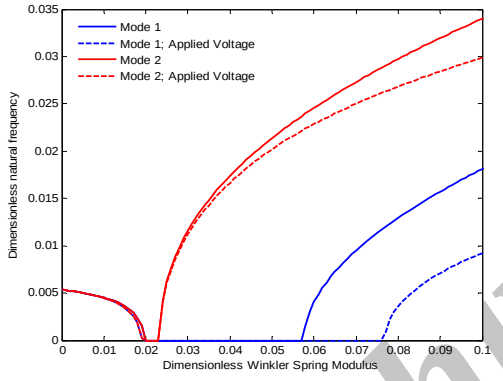

Fig. 8
Effect of applying electric potential on natural frequency with changing Winkler modulus for 1st and 2nd mode.

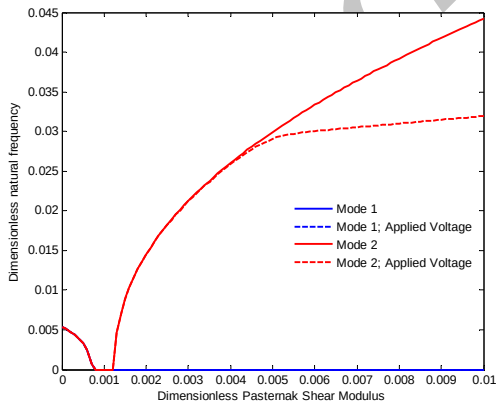

Fig. 9
Effect of applying electric potential on natural frequency with changing Pasternak modulus for 1st and 2nd mode.

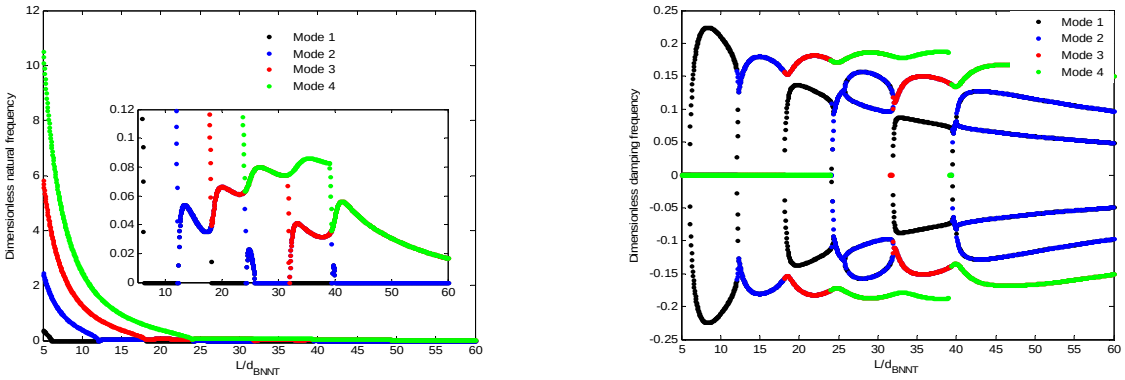

(a) (b)

Fig. 10
a) Dimensionless natural frequency versus aspect ratio for 1st to 4st mode. b) Dimensionless damping frequency versus aspect ratio for 1st to 4st mode.

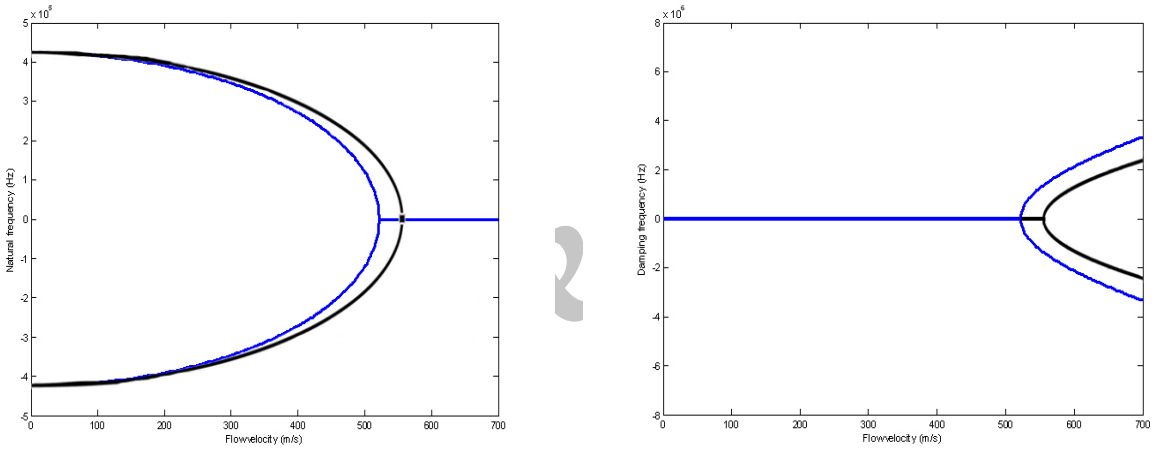

(a) (b)

Fig. 11
a) Comparison of the dimensionless natural frequency versus dimensionless flow velocity for simplified analysis of the present work and Ref. [21]. b) Comparison of the dimensionless damping frequency versus dimensionless flow velocity for simplified analysis of the present work and Ref. [21].

7 CONCLUSION

Flow-induced instability of a CDNTS, consisting BNNT and CNT which are coupled by Pasternak media has been studied in this article. Nonlocal elasticity theory for stress and electric displacement has been implemented. Polynomial modal expansions for components of displacement and electric potential have been employed to obtain equations of motion. Effects of various parameters including small-scale, fluid-scale, aspect ratio and etc. have been studied and incredible role of the BNNT for controlling stability of the fluid-conveying CNT by elastic media existed between the nanotubes and external applied voltage have been observed in this regard. Indeed ,applications of CDNTS can proper flow-induced instability and use as sensors and actuators in nano-electro-mechanical systems.

ACKNOWLEDGMENTS

The authors are grateful to University of Kashan for supporting this work by Grant No. 65475/57.

REFERENCES

[1] Vaccarini L., Goze C., Henrard L., Herna´ndez E., Bernier P., Rubio A., 2000, Mechanical and electronic properties of carbon and boron–nitride nanotubes, *Carbon* **38**: 1681–1690.

[2] Lahiri D., Rouzaud F., Richard T., Keshri A.K., Bakshi S.R., Kos L., Agarwal A., 2010, Boron nitride nanotube reinforced polylactide–polycaprolactone copolymer composite: Mechanical properties and cytocompatibility with osteoblasts and macrophages in vitro, *Acta Biomaterialia* **6**: 3524-3533.

[3] Ghorbanpour Arani A., Shajari A.R., Atabakhshian V., Amir S., Loghman A., 2013, Nonlinear dynamical response of embedded fluid-conveyed micro-tube reinforced by BNNTs, *Composites Part B* **44**: 424–432.

[4] Ghorbanpour Arani A., Shajari A.R., Amir S., Loghman A., 2012, Electro-thermo-mechanical nonlinear nonlocal vibration and instability of embedded micro-tube reinforced by BNNT, conveying fluid, *Physica E* **45**: 109-121.

[5] Salehi-Khojin A., Jalili N., 2008, Buckling of boron nitride nanotube reinforced piezoelectric polymeric composites subject to combined electro-thermo-mechanical, *Loadings Composites Science and Technology* **68**: 1489-1501.

[6] Ghorbanpour Arani A., Atabakhshian V., Loghman A., Shajari A.R., Amir S., 2012, Nonlinear vibration of embedded SWBNNTs based on nonlocal Timoshenko beam theory using DQ method, *Physica B* **407**: 2549-2555.

[7] Kuang Y.D., He X.Q., Chen C.Y., Li G.Q., 2009, Analysis of nonlinear vibrations of double-walled carbon nanotubes conveying fluid, *Computation Materials Science* **45**: 875-880.

[8] Fu Y.M., Hong J.W., Wang X.Q., 2006, Analysis of nonlinear vibration for embedded carbon nanotubes, *Journal of Sound and Vibration* **296**: 746-756.

[9] Narasimhan M.N.L., 2010, On the flow of an electrically conducting nonlocal viscous fluid in a circular pipe in the presence of a transverse magnetic field in magneto hydro dynamics, *International Journal of Fluid Mechanics Research* **37** (2): 190-199.

[10] Vu H.V., Ordonez A.M., Karnopp B.H., 2000, Vibration of a double-beam system, *Journal of Sound and Vibration* **229** (4): 807-822.

[11] Lin Q., Rosenberg J., Chang D., Camacho R., Eichenfield M., Vahala K.J., Painter O., 2010, Coherent mixing of mechanical excitations in nano-opto-mechanicalstructures, *Nature Photonics* **4**: 236-242.

[12] Murmu T., Adhikari S., 2010, Nonlocal effects in the longitudinal vibration of double-nanorod systems, *Physica E* **43**: 415-422.

[13] Ke L.L., Wang Y.Sh., Wang Zh.D., 2012, Nonlinear vibration of the piezoelectric nanobeams based on the nonlocal theory, *Composite Structures* **94**: 2038-2047.

[14] Han J.H., Lee I., 1998, Analysis of composite plates with piezoelectric actuators for vibration control using layerwise displacement theory, *Composites Part B* **29**: 621-632.

[15] Reddy J.N., 2004, Wang C.M., *Dynamics of Fluid Conveying Beams: Governing Equations and Finite Element Models*, Centre for offshore research and engineering national university of singapore.

[16] Rashidi V., Mirdamadi H.R., Shirani E., 2012, A novel model for vibrations of nanotubes conveying nanoflow, *Computation Materials Science* **51**: 347-352.

[17] Shokouhmand H., Isfahani A.H.M., Shirani E., 2010, Friction and heat transfer coefficient in micro and nano channels filled with porous media for wide range of Knudsen number, *International Communications in Heat and Mass Transfer* **37**: 890-894.

[18] Ke L.L., Yang J., Kitipornchai S., 2010, Nonlinear free vibration of functionally gradedcarbon nanotube-reinforced composite beams, *Composite Structures* **92**: 676-683.

[19] Nirmala V., Kolandaivel P., 2007, Structure and electronic properties of armchair boron nitride nanotubes, *Journal of Molecular Structure: Theochem* **817**: 137-145.

[20] Yang, J. Ke L.L., Kitipornchai S., 2010, Nonlinear free vibration of single-walled carbonnanotubes using nonlocal Timoshenko beam theory, *Physica E* **42**: 1727-1735.

[21] Kaviani F., Mirdamadi H.R., 2012, Influence of Knudsen number on fluid viscosity for analysis of divergencein fluid conveying nano-tubes, *Computation Materials Science* **61**: 270-277.